

Supporting Information

Cyclic Voltammograms of n^{++} Si/Ti/TiO₂/Pt without the Fe(II)/Fe(III) redox couple

For completeness, cyclic voltammograms were taken of the n^{++} Si/ 5 nm Ti/ 100 nm TiO₂/Pt in Ar purged 1M HClO₄. The electrodes were scanned from 2.6 V vs. RHE to -0.04 V vs. RHE at a scan rate of 20mV/s. This experiment was identical to the experiment done in Figure 2 of the main paper, except that there was no Fe(II)/Fe(III) redox couple in solution. Figure S1 shows the CV of both the unannealed and vacuum annealed sample, while the inset is a magnification of the CV's in the low current regime.

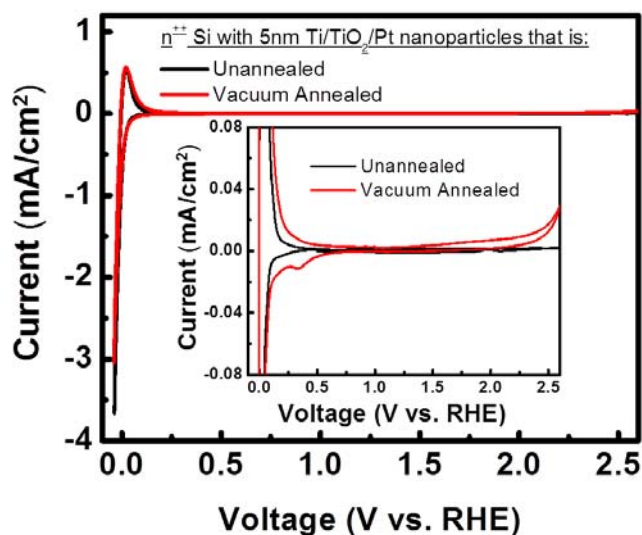


Figure S1: Cyclic voltammograms of n^{++} Si/ 5 nm Ti/ 100 nm TiO₂/Pt Si in an argon purged 1.0 M HClO₄ aqueous solution containing.

Comparing Figure S1 to Figure 2 in the main paper, Figure S1 has both the H⁺/H₂ reduction and oxidation peak as in Figure 2. The inset shows the unannealed sample has no other peaks. Interestingly the vacuum annealed sample does show a couple of small peaks. At 0.3V vs. RHE there is a very slight cathodic current. While in the main paper, this was attributed to Fe(III) reduction, there is no Fe(III) in this solution. In this case this current can be attributed to the standard hydrogen underdeposition that is seen when cycling platinum. It is important to note that in Figure S1 the current at 0.3V vs. RHE is approximately 20 times smaller than the case where Fe(III) was in the electrolyte. This allows us to verify that the majority of current at 0.3V vs. RHE in the main paper is due to Fe(III) reduction. The point of this work is to show that electronic tunneling from the TiO₂ to the surface can occur in the vacuum annealed sample. In the main paper this is shown by these electrons reducing Fe(III) and in Figure S1 this can be seen via electrons coming to the surface for hydrogen underdeposition.

The other interesting peak on the vacuum annealed sample is the peak at 2.6V vs. RHE. At this potential it appears as if electrons can tunnel through the TiO₂ from the Pt due to water oxidation (oxygen evolution). Again this current is much smaller than the current at 2.6V vs. RHE in Figure 2 of the main paper where Fe(II) was being oxidized. This verifies that the majority of the current in Figure 1 can be attributed to Fe(II) oxidation.

Effective Density of States in the Conduction Band (N_c) Calculations

Effective density of states in the conduction band (N_c) can be calculated using Equation 1:

$$N_c = 2 \left[\frac{2\pi m_{\text{eff}} kT}{h^2} \right]^{\frac{3}{2}} \quad \text{Equation 1}$$

In this equation m_{eff} is the effective mass of the electron in the TiO₂. In this work a m_{eff} of 10 m_0 is used for N_c calculations¹, where m_0 is the mass of a free electron. k is the Boltzmann constant, h is the Planck constant and T is the semiconductor temperature (298K). By applying Equation 1, N_c is determined to be $7.8 \times 10^{20} \text{ cm}^{-3}$.

Electronic Tunneling Calculations

To determine what tunneling currents should be expected between the TiO₂ and the Fe(II)/Fe(III) redox couple, electronic tunneling calculations need to be employed. Since the energy barrier due to band bending at a semiconductor/electrolyte closely resembles a triangle, the tunneling probability can be described via a triangular barrier. By using the Wentzel-Kramers-Brillouin (WKB) approximation the tunneling probability (T_t) is given by Equation 2²:

$$T_t = \exp \left[-\frac{4}{3} \Delta x \sqrt{\frac{2m_{\text{eff}}q\phi_b}{\hbar^2}} \right] \quad \text{Equation 2}$$

In this equation \hbar is Planck's constant divided by 2π , q is the elementary charge, ϕ_b is the barrier height and Δx is barrier width, i.e. the tunnel distance. The barrier height is simply the difference in applied potential versus the conduction band. For the case of the Fe(II)/Fe(III) redox couple, the tunnel distance is approximately the depletion width at potentials more cathodic than the Fe(II)/Fe(III) redox potential. At potentials more anodic than the Fe(II)/Fe(III) redox couple, the tunnel distance is the distance into the TiO₂ where the conduction band is at the Fe(II)/Fe(III) redox potential. Since both ϕ_b and Δx vary with applied potential, the tunneling probability will also vary with applied potential.

Equation 3 allows one to determine the tunneling current density (J_t) that will occur at a given tunneling probability²:

$$J_t = -N_C v_{\text{th}} q T_t \quad \text{Equation 3}$$

In this equation v_{th} is the thermal velocity ($\sim 10^7$ cm/s at room temperature). Since both T_t and N_C are a function of m_{eff} , any variation in m_{eff} can greatly influence tunneling current. Different authors have found m_{eff} values from 0.77-30 m_0 ³⁻⁷ for anatase TiO₂ with the trend that higher m_{eff} are seen in nanoparticles¹ while lower m_{eff} are seen in bulk TiO₂ situations^{4,7}. Given that the origin of these discrepancies are still debated and not fully understood, it is not straightforward to accurately determine what the expected tunneling current should be. However, using the lower end of these values allows for tunneling current density on the range of μA to mA that is seen in Figure 2.

1. B. Enright and D. Fitzmaurice, *Journal of Physical Chemistry*, 1996, **100**, 1027-1035.
2. K. N. Kwok, *Complete Guide to Semiconductor Devices*, McGraw-Hill, New York, 1995.
3. M. A. Henderson, *Surface Science Reports*, 2011, **66**, 185-297.
4. Y. X. Weng, Y. Q. Wang, J. B. Asbury, H. N. Ghosh and T. Q. Lian, *Journal of Physical Chemistry B*, 2000, **104**, 93-104.
5. H. Tang, K. Prasad, R. Sanjines, P. E. Schmid and F. Levy, *Journal of Applied Physics*, 1994, **75**, 2042-2047.
6. C. Kormann, D. W. Bahnemann and M. R. Hoffmann, *Journal of Physical Chemistry*, 1988, **92**, 5196-5201.
7. M. D. Stamate, *Applied Surface Science*, 2003, **205**, 353-357.